---

**Article:**
Nedelkoski, Zlatko, Do Nascimento, Julio A., Hamaya, Kohei et al. (1 more author) (2025) Effects of atomic structures at Co2Fe(Al0.5,Si0.5)/Ge interfaces on spin-electronic properties. Journal of Physics D: Applied Physics. 245301. ISSN 0022-3727

https://doi.org/10.1088/1361-6463/addd2d

---

Journal of Physics D:
Applied Physics



**PAPER** • **OPEN ACCESS**

# Effects of atomic structures at $Co_2Fe(Al_{0.5},Si_{0.5})$/Ge interfaces on spin-electronic properties

To cite this article: Zlatko Nedelkoski *et al* 2025 *J. Phys. D: Appl. Phys.* **58** 245301



OPEN ACCESS
IOP Publishing
Journal of Physics D: Applied Physics
J. Phys. D: Appl. Phys. **58** (2025) 245301 (8pp)
https://doi.org/10.1088/1361-6463/addd2d

# Effects of atomic structures at $Co_2Fe(Al_{0.5},Si_{0.5})$/Ge interfaces on spin-electronic properties

**Zlatko Nedelkoski[1], Julio A Do Nascimento[2], Kohei Hamaya[3] and Vlado K Lazarov[2,*]**

[1] Faculty of Technical Sciences, Mother Theresa University, 1669 11A, Skopje, North Macedonia
[2] Department of Physics, University of York, Heslington, YO10 5DD York, United Kingdom
[3] Center for Spintronics Research Network, Graduate School of Engineering Science, Osaka University, 1-3 Machikaneyama, Toyonaka 560-8531, Japan

E-mail: vlado.lazarov@york.ac.uk

Received 12 February 2025, revised 20 May 2025
Accepted for publication 26 May 2025
Published 4 June 2025

**Abstract**

Efficient spin injection is essential for the development of ferromagnet—semiconductor spintronic devices with high performances, including spin transistors. Although the $Co_2Fe(Al_{0.5},Si_{0.5})$ (CFAS)/Ge hybrid structure has been identified as an outstanding platform for such devices, there is a lack of systematic analyses on the effects of the interface atomic structure on the spin-electronic properties. In this study, we investigate electronic and magnetic properties of CFAS/Ge (001) interfaces by density functional theory calculations under two possible scenarios, with atomically abrupt bulk-like interfaces and with intermixing at the interfaces. For two possible terminations in the case of abrupt interfaces, we show considerable reductions in spin polarization (SP), which is emphasized in the case of the —Fe—Si,Al/Ge interface, where the SP has reversed sign. Further, we show that Fe—Ge interdiffusion is most likely to occur at the interface, and that this intermixing does not largely affect the spin-electronic properties. In contrast, the model of interdiffusion affecting the Co sublattice in the CFAS film exhibits a reversed SP at the interface layers, but this is less likely to occur owing to the higher energy for such atomic swaps. Band alignment analyses show that interfaces with a small degree of Fe/Ge intermixing could be beneficial for the spin injection efficiency. This study demonstrates that the spin injection efficiency is strongly dependent on the ferromagnet—semiconductor interface atomic structure, and thus can guide further theoretical and experimental studies for development of spintronic devices with improved properties.

Supplementary material for this article is available online

Keywords: density functional theory, spintronics, spin injection, Heusler alloys, $Co_2Fe(Al_{0.5},Si_{0.5})$

* Author to whom any correspondence should be addressed.

## 1. Introduction

Co-based full Heusler alloys are important functional materials for applications in advanced electronic and spintronic devices owing to their desirable spin-electronic structures [1–4]. Numerous materials of this class, including $Co_2MnSi$, $Co_2FeSi$, and $Co_2Fe(Al_{0.5},Si_{0.5})$ (CFAS), have been predicted to be 100% spin-polarized by density functional theory (DFT) calculations, and thus have garnered considerable interest over the past years for spintronic applications including spin valve structures on Ge [5] and Si [6]. Among them, CFAS has been of particular interest due to its position of the Fermi level in the middle of the band gap of the minority spin-down electrons, abundance of its constituent elements, and very high Curie temperature (∼1000 K) [7]. The suitable Fermi level position makes this material more robust against temperature effects [7], which are inevitable in real application scenarios, while the abundance of its elements could enable a lower cost of production of devices based on CFAS.

Co-based full Heusler alloys have already been employed in numerous heterostructured spintronic devices [8–12]. However, the measured performances of such devices have often been considerably lower than those predicted for ideal bulk-like structures. The weakened properties have been attributed to disorder, deviation from the ideal stoichiometry, strain, and extended structural defects in the Heusler alloy thin films [13–15]. In addition to such effects from the interior of the film, the devices can suffer from effects originating from undesirable structures at their interfaces, between thin films and/or between thin films and substrate [16, 17]. This can lead to a decrease in the local spin polarization (SP), which, in turn, reduces the magnetoresistance for spin valve devices or efficiency of spin injection from the spin-polarized electrode into a semiconductor such as Si, Ge, and GaAs.

Thus, the realization of atomic control at heterointerfaces is crucial to engineer various electronic properties including the SP, interfacial magnetism, Schottky barrier height, band alignment, and interface conductivity. However, this is still rather challenging considering the chemical intermixing by interdiffusion and interface strain due to the lattice mismatch between the film and substrate. In addition, the conductivity mismatch between the ferromagnet film and semiconductor substrate hinders an efficient spin injection, a problem that could be addressed by using 100% spin-polarized materials at the Fermi level as ferromagnetic electrodes [18]. CFAS could be an ideal candidate for such applications considering its predicted 100% SP and mid-gap Fermi level, which could provide a robust structure for novel low-electric-power high-efficiency spin-electronic devices.

However, the interface between CFAS and mainstream semiconductor Si suffers from a strong out-diffusion of Si, relatively large lattice mismatch of ∼4.5% between CFAS and Si, and formation of nonmagnetic thermodynamically stable phases (Co and Fe silicides) in a relatively thick ∼3 nm region [16, 17]. These factors hinder a widespread use of the CFAS/Si heterostructure for spintronic applications.

These issues have been largely mitigated by the use of Ge as a substrate. It reduces the lattice mismatch to only 0.2%, largely reduces the diffusion of substrate atoms into the film, and prevents the formation of undesirable secondary phases at the interface [19]. Thus, the CFAS/Ge hybrid structure provides an efficient platform for development of devices with excellent properties [20, 21]. Although this structure has been experimentally realized, a systematic computational analysis on the effects of the interface atomic structure on the spin-electronic structures is lacking.

In this study, we analyze electronic and magnetic properties of CFAS/Ge (001) interfaces by DFT calculations under two scenarios, with atomically abrupt bulk-like interfaces and with intermixing at the interfaces. We demonstrate that, for the two possible terminations in the case of abrupt interfaces, there are large reductions in SP, particularly in the case of the —Fe–(Si,Al)/Ge interface, where the SP sign is reversed. Further, we show that Fe–Ge interdiffusion is most likely to occur at the interface. However, this intermixing does not largely affect the spin-electronic properties. In contrast, the interdiffusion affecting the Co sublattice in the CFAS film reverses the SP at the interface layers, but this type of disorder is less likely to occur owing to the higher energy for such atomic swaps. Moreover, by band alignment analyses, we show that interfaces with a small degree of Fe/Ge intermixing may be even beneficial for the spin injection efficiency.

## 2. Methods

We carried out all DFT calculations by the CASTEP [22] code on supercells constructed using two CFAS and two Ge interfaced unit cells along the [001] crystallographic direction with approximately 10 Å thick vacuum region to enable simulations of the effects at the interfaces. The supercells are periodic in the in-plane directions. In the interior parts of both CFAS and Ge, we recover the bulk-like electronic structures, which justifies the choice of the supercell dimensions. All atomic coordinates at the interface region were geometrically optimized. We employed the Perdew–Burke–Ernzerhof (PBE) + $U$ exchange–correlation functional with a Hubbard $U$ value of 2.1 eV for both $d$-block elements, Co and Fe [23], which opens up the minority band gap, and approximately corrects for the delocalization effect of self-interaction with the use of the PBE functional alone [24]. Ultrasoft PBE pseudopotentials with a plane wave cut-off energy of 400 eV were employed. We sampled the Brillouin zone with a Monkhorst–Pack grid with a $k$-point sampling spacing of 0.035 $2\pi$Å$^{-1}$. The valence band edges were computed separately for bulk CFAS and Ge with respect to their averaged potentials, and offset for the calculated potential difference across the interface [17, 25]. The potential is the sum of the local part of the pseudo-potential, Hartree term, and exchange term. It was averaged in-plane and plotted along the direction normal to the interface plane. Partial densities of states (PDOSs) were computed with the OPTADOS [26] code using fixed Gaussian broadening. The

VESTA program was used for visualization of the atomic structures [27].

## 3. Results and discussion

We investigated five different interface supercell models, which are schematically illustrated in figure 1(a). The supercell consists of two CFAS and two Ge unit cells interfaced along the [001] crystallographic direction on a (001) atomic plane. The atomic structure of CFAS is illustrated in supplementary figure S1 along different viewing directions. The in-plane strain effects for this heterostructure could be neglected considering the very small lattice mismatch between Ge and CFAS (0.2%) and robustness of the CFAS electronic structure (e.g., the minority band gap is not destroyed even under a strain up to 5%, as illustrated in supplementary figure S2). A similar trend has been observed in Fe-based Heusler alloys [28]. The dimensions of the supercells are sufficient to recover the bulk-like spin-electronic properties away from the interface plane, as shown in figure 1(b), where we plot spin-polarized PDOSs for different layers parallel to the interface in the interior parts of both CFAS film and Ge substrate.

The five plots show the successful recovery of the bulk-like properties away from the interface including the appearance of the band gap in Ge, and band gap and metallic state for the spin-down and spin-up electrons in CFAS, respectively. The bulk-like electronic structures in the regions away from the surfaces and interface in supplementary figure S3 further demonstrate that the surface effects do not affect the interfacial properties of the CFAS/Ge(100) heterostructure. Further expansion of the supercell dimensions in the direction normal to the interface would lead to considerably longer calculations considering the large number of different atoms in our models. Thus, to a good extent, these dimensions of the supercells are sufficient for a suitable analysis of the interfacial properties.

Further, we investigate the electronic properties for two different interface structures without interdiffusion of elements, characterized by —Fe–Si/Ge (denoted as i1) and —Co/Ge (denoted as i2) termination layer structures, as shown in figures 2(a) and (c), respectively. We investigate the electronic properties for three successive layers at these interfaces, denoted as L1, L2, and L3, with atom structures presented in table 1 and illustrated in figure 2. The spin-polarized PDOSs in figure 2 show the significant changes in the electronic structure at the interfacial layers compared to that in the interior (bulk-like) part of the film. We calculated the SPs for the three layers for both structures i1 and i2, as shown in table 1, using the formula $\mathrm{SP} = (\mathrm{PDOS}_u - \mathrm{PDOS}_d)/(\mathrm{PDOS}_u + \mathrm{PDOS}_d)$, where $\mathrm{PDOS}_u$ and $\mathrm{PDOS}_d$ are the PDOSs for the spin-up and -down electrons at the Fermi level, respectively. As shown by the plots in figure 2 and values in table 1, the specific configurations at both interfaces lead to states at the Fermi level for the minority (spin down) electrons, which are not present in the bulk-like parts of the film. This effect is more emphasized for the i1 structure, which becomes inversely, i.e., negatively, spin-polarized at the interface, with values reaching $-62\%$ at the first interface layer. The behavior for the i2 termination is notably different. This structure generally preserves the SP, except for a slight reversal at the first interface layer with SP of $-11\%$. However, the next atomic layer in the CFAS part has a relatively large positive value of $+41\%$. The states at the Fermi level for the minority electrons are detrimental for the overall performance of the considered hybrid system, as they largely affect the local SP, and thereby would reduce the spin injection efficiency of a device based on this structure.

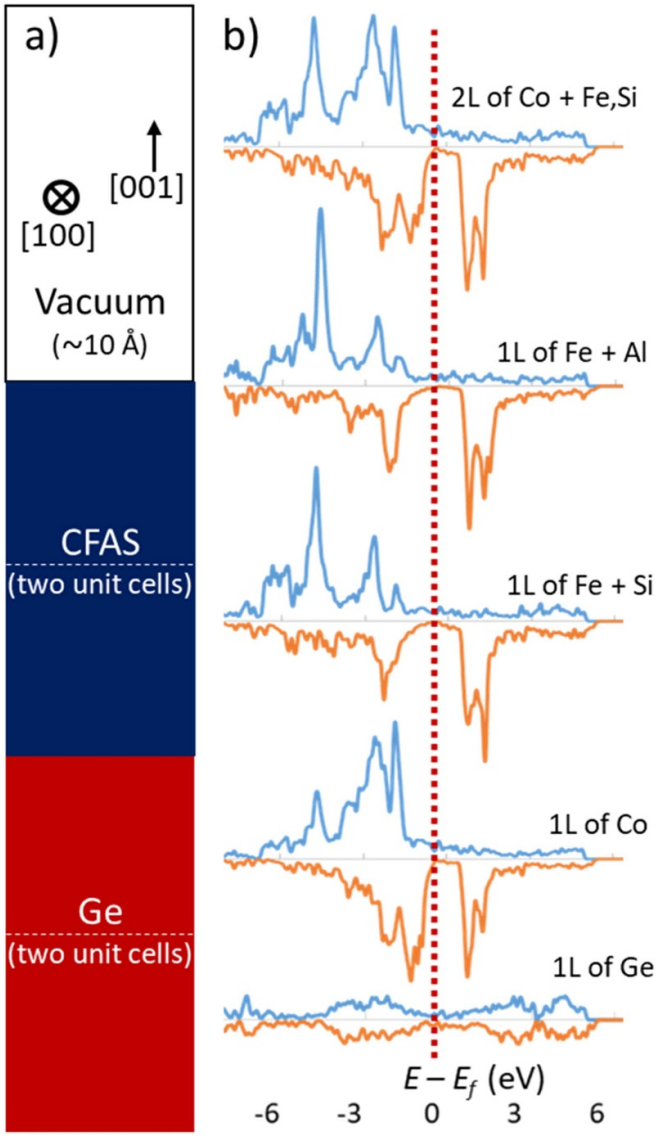


**Figure 1.** (A) Schematic of the supercell structure and (b) PDOSs in the bulk-like parts of the supercell. The position of the Fermi level is denoted by the red dotted line. The five presented plots correspond to the following layers (parallel to the interface plane): 1L of Ge (one atomic layer of Ge in the interior of the substrate), 1L of Co (one atomic layer of Co in the interior of CFAS), 1L of Fe + Si (one atomic layer including both Fe and Si in the interior of CFAS), 1L of Fe + Al (one atomic layer including both Fe and Al in the interior of CFAS), and 2L of Co + Fe,Si (two atomic layers including one Co plane and another plane with Fe and Si atoms). The PDOSs are presented in relative units as a function of the energy difference from the Fermi level. The plots in the top panels (blue line) are for the spin-up electrons, while those in the bottom panels (orange line) are for spin-down electrons.

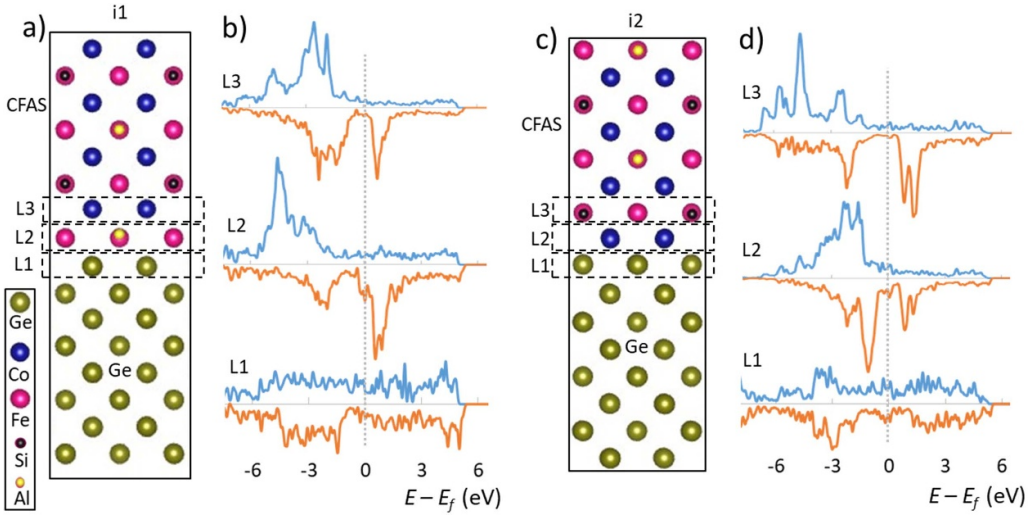


**Figure 2.** Supercell models with abrupt terminations without intermixing, (a) —Fe–Si/Ge (denoted as i1) and (c)—Co/Ge (denoted as i2), and (b), (d) their PDOSs for three layers in the vicinity of the interfaces defined by the dashed rectangles in (a), (c), respectively. The atom color coding is indicated in the legend.

**Table 1.** Spin-electronic and magnetic properties at the different interfaces without interdiffusion. In the first three rows, we show the types of atoms in the layers at the vicinity of the interface. In the next three rows, we show their SPs. $m_{L1/2/3}$ denote the spin magnetic moments for the different atoms in the interface layers. $\Delta V_u$ and $\Delta V_d$ are the local potential differences across the interfaces for spin-up and -down electrons, respectively.

| | i1 | i2 |
|---|---|---|
| L1 atoms | Ge | Ge |
| L2 atoms | Fe, Al | Co |
| L3 atoms | Co | Fe, Si |
| $SP_{L1}$ (%) | 8 | 13 |
| $SP_{L2}$ (%) | −62 | −11 |
| $SP_{L3}$ (%) | −17 | 41 |
| $m_{L1}$ ($\mu_B$/atom) | Ge: −0.05 | Ge: −0.08 |
| $m_{L2}$ ($\mu_B$/atom) | Fe: 3.19<br>Al: −0.18 | Co: 1.02 |
| $m_{L3}$ ($\mu_B$/atom) | Co: 1.14 | Fe: 3.06<br>Si: −0.13 |
| $\Delta V_u$ (eV) | 4.97 | 5.27 |
| $\Delta V_d$ (eV) | 4.77 | 5.09 |

Further, we calculated the local spin magnetic moments for all atoms at the interfacial layers, as presented in table 1. We performed such calculations also for the interior of the CFAS film, where we obtained the following values of magnetic moment for the different atoms: Co: 1.22 $\mu_B$, Fe: 3.19 $\mu_B$, Al: −0.19 $\mu_B$, and Si: −0.07 $\mu_B$. According to the results in table 1, both Co and Fe have slightly reduced magnetic moments in i1 compared to the bulk, while more notable reductions are obtained for the i2 structure. However, the changes are relatively small for both cases, and thus are not expected to lead to significant changes in overall magnetic properties.

To estimate the probability of intermixing at these interfaces, we calculated the energy differences for atomic swaps, which can arise from the interdiffusion of the different atoms between the film and substrate. Although the models of interdiffusion are simplified, the calculated results are in line with previous observations [19]. Regarding the i1 structure, the difference in energy between the interface with interdiffusion of Ge and Fe and that without interdiffusion is approximately −0.54 eV/supercell, while the value for interdiffusion of Ge and Al is 0.75 eV/supercell. On the other hand, for the i2 structure, the difference in energy between the interface with interdiffusion of Ge and Co and that without interdiffusion is approximately 1.64 eV/supercell (table 2). This is consistent with our previous energy-dispersive spectroscopy (EDS) measurement on the CFAS/Ge (111) hybrid system [19], which showed very sharp suppressions of Al/Si EDS signals in the Ge substrate part, reflecting the low probability of diffusion, which is likely attributed to their large difference in size with respect to Ge. Even sharper suppression has been observed for the Co EDS signal, consistent with the above calculated energy difference. On the other hand, Fe and Ge gradually interdiffused across a region of several nanometers according to the EDS signals, which also is consistent with the calculated energy differences, indicating that the interface with interdiffusion is energetically more stable than the atomically abrupt interface.

Notably, these findings suggest that the interface tends to be depleted mostly in Fe among the CFAS elements. In a recent study, an additional thin Fe layer has been introduced at the interface between CFAS and Ge to address the conductivity mismatch issue, and an efficient spin injection has been realized. In other words, the interface has been enriched in Fe, which addresses the likely Fe depletion

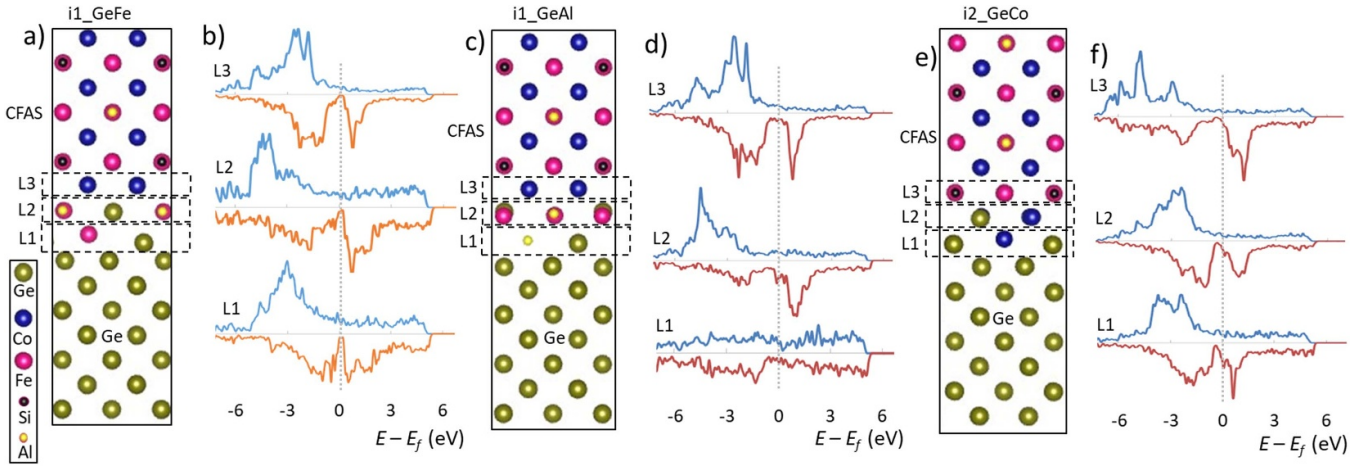


**Figure 3.** Supercell models with intermixing at the interface: (a) i1 termination with intermixing of Ge and Fe (denoted as i1_GeFe), (c) i1 termination with intermixing of Ge and Al (denoted as i1_GeAl), (e) i2_termination with intermixing of Ge and Co (denoted as i2_GeCo), and (b), (d), (f) their PDOSs for three layers in the vicinity of the interfaces defined by the dashed rectangles in (a), (c), (e), respectively.

in the heterointerface structures between CFAS and Ge. It can be expected that the symmetry matching of the electronic bands between the top highly spin polarized CFAS and semiconductor is preserved with Fe–Ge intermixing, according to the spin signal for a lateral spin-valve device enhanced by up to one order of magnitude compared to that obtained with a conventional ferromagnet/semiconductor structure [29]. These results further demonstrate the importance of tailoring the structure at the interface at atomic scale, where even subtle differences could provide largely improved performances.

The atomic structures and resultant spin-polarized PDOSs for the considered interfaces with interdiffusion of elements are shown in figure 3. The plots as well as the calculated values in table 2 show that the i1 structure with Ge–Fe interdiffusion, which, according to the calculations, is most likely to form at the interface, exhibits relatively large SP values at the three layers, without reversal of SP. Notably, at least approximately 50% of SP is retained in all layers. Thus, the likely interdiffusion between Fe and Ge is not expected to largely affect the spin-electronic properties. In the case with interdiffusion between Ge and Al, which is less likely, the SP is largely reduced and even reversed in one atomic layer. The behavior for the interface with interdiffusion between Ge and Co is even worse in terms of SP, which is negative in all three layers, with relatively large values reaching even −40%. The disorder in the Co sublattice has also been previously identified as detrimental for the SP of the Heusler alloy electrode. However, according to the calculated formation energies and reported EDS profiles and maps [19], this type of disorder is less likely at the interface. In terms of magnetism, table 2 shows that the local atomic magnetic moments at these interfaces are not considerably different from those in the bulk-like parts of the CFAS film. Reduced SP or even spin reversal as well as notable changes in magnetic moments near interfaces have also been previously calculated for other Heusler alloy heterostructures [30]. In contrast to the slight changes in magnetic moments around the interface for this heterostructure, which have been also demonstrated experimentally for the (111) type of CFAS/Ge interface [19], a magnetically inactive region has been predicted by calculations and demonstrated experimentally for a CFAS/Si heterostructure [17, 31], which exhibits secondary phases at the interface, largely reducing the magnetic moment as well as the local SP.

In general, the band alignment at the interfaces strongly correlates with their atomic structures, and, for the case of spin injector and semiconductor (in our case, CFAS/Ge), is

**Table 2.** Spin-electronic and magnetic properties at the different interfaces with interdiffusion. The quantity notation is as in table 1. $E_d$ is the difference in energy between an interface with interdiffusion and corresponding bulk-like-terminated interface without interdiffusion. A negative value indicates that the interface with interdiffusion is energetically more stable than the corresponding without interdiffusion.

| | i1_GeFe | i1_GeAl | i2_GeCo |
|---|---|---|---|
| L1 atoms | Ge, Fe | Ge, Al | Ge, Co |
| L2 atoms | Fe, Ge, Al | Fe, Al, Ge | Co, Ge |
| L3 atoms | Co | Co | Fe, Si |
| $SP_{L1}$ (%) | 49 | 6 | −39 |
| $SP_{L2}$ (%) | 52 | −36 | −38 |
| $SP_{L3}$ (%) | 77 | 3 | −20 |
| $m_{L1}$ ($\mu_B$/atom) | Ge: −0.10<br>Fe: 2.41 | Ge: −0.08<br>Al: −0.09 | Ge: −0.03<br>Co: 1.45 |
| $m_{L2}$ ($\mu_B$/atom) | Ge: −0.02<br>Fe: 3.03<br>Al: −0.18 | Ge: −0.04<br>Fe: 3.20<br>Al: −0.18 | Ge: −0.03<br>Co: 1.47 |
| $m_{L3}$ ($\mu_B$/atom) | Co: 1.06 | Co: 1.17 | Fe: 3.08<br>Si: −0.06 |
| $\Delta V_u$ (eV) | 5.34 | 5.40 | 5.40 |
| $\Delta V_d$ (eV) | 5.15 | 5.21 | 5.18 |
| $E_d$ (eV/supercell) | −0.54 | 0.75 | 1.64 |

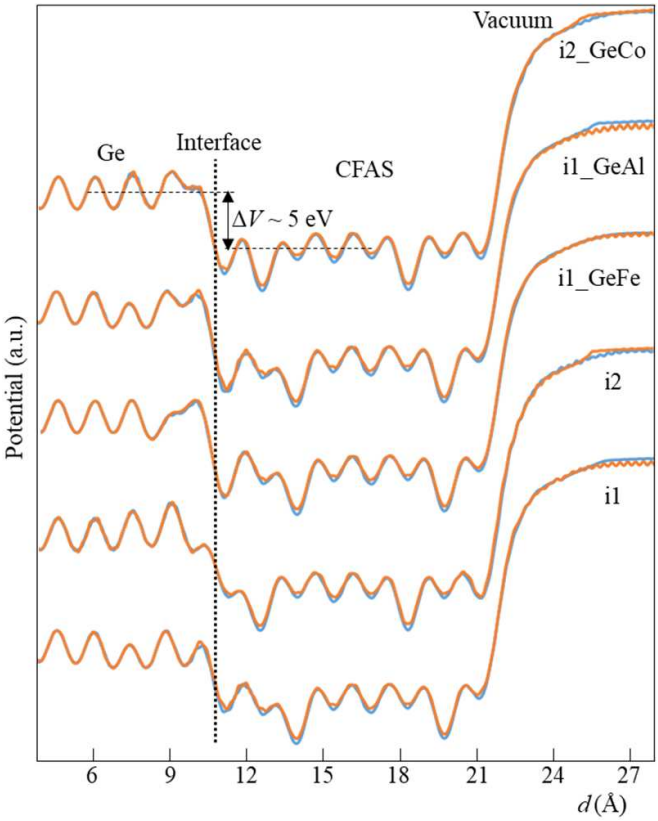


**Figure 4.** In-plane-averaged local potentials across the supercells as a function of the distance from the bottom plane (blue curve: spin-up electrons, red curve: spin-down electrons).

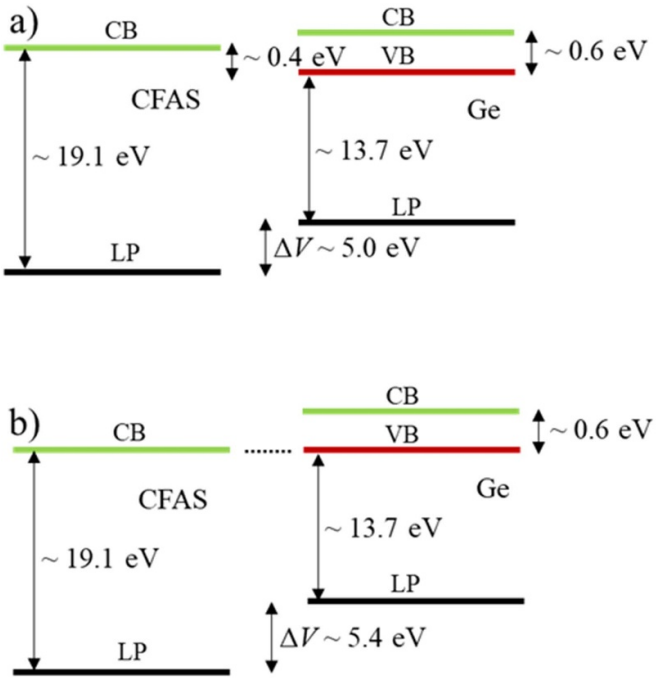


**Figure 5.** Band alignment for the majority spin-up electrons: (a) abrupt i1 structure, (b) i2_GeCo structure with interface mixing. CB: conduction band, VB: valence band, LP: local potential.

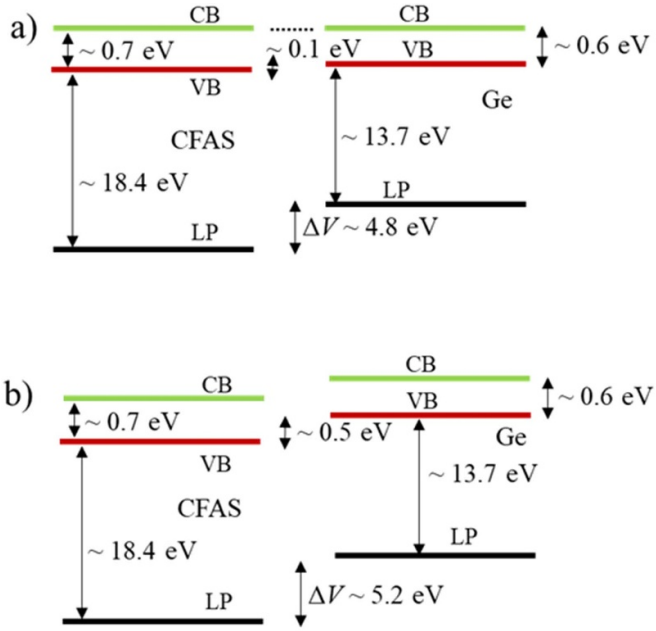


**Figure 6.** Band alignment for the minority spin-down electrons: (a) abrupt i1 structure, (b) i2_GeCo structure with interface mixing.

rather important for an efficient spin injection [29]. To elucidate the band alignment for this hybrid system, we calculated the local potentials for all supercell models, as the sum of the local part of the pseudo-potential, Hartree term, and exchange term. The calculated potentials were then averaged in-plane and analyzed along the direction normal to the interface plane (figure 4) for both spin-up and spin-down electrons.

There are clear drops in potential for all interface models on the order of 5 eV. The calculated values are presented in tables 1 and 2. For all models, we obtained a difference in potential difference across the interface plane between the spin-up and spin-down electrons of approximately 0.2 eV due to the spin-polarized structure of the CFAS electrode. The smallest potential difference is obtained for the abrupt i1 structure, which gradually increases up to the largest value obtained for the structure with interdiffusion of Ge and Co. We employed these potential profiles to compute the positions of the valence band edges for the supercell models. The valence band edges were computed separately for bulk CFAS and Ge with respect to their averaged potentials, and then offset for the calculated potential difference across the interface [17, 25].

The obtained valence band edge positions were then employed to investigate the band alignment of these interfaces. Figures 5 and 6 illustrate the calculated band alignments for the majority spin-up electrons and minority spin-down electrons, respectively, for two interface models, i1 with the smallest potential difference and i2_GeCo with the largest potential difference. The potentials of the other interface models are between these two extreme cases, and thus we focused only on the limiting cases for simplicity of the analysis.

As shown in figure 5 for the majority electrons, in the case of the i1 abrupt structure, the conductance band edge position, which is identical to the valence band edge position considering the metallic-like spin-up state of CFAS, is positioned

approximately in the middle of the band gap of the Ge substrate. Therefore, there is a potential barrier of approximately 0.2 eV to overcome for an injection of the spin-up electrons into the Ge substrate. In addition to the locally reduced SP, the spin injection efficiency is expected to be negatively affected by this potential difference.

On the other hand, for the i2_GeCo structure, the position of the conduction band edge of CFAS is identical to that of the valence band edge of the Ge substrate. This implies that the spin-up electrons from CFAS have to overcome a considerably larger barrier equal to the band gap width of Ge to be efficiently injected. Therefore, we expect that this type of interdiffusion would largely reduce the spin injection current.

However, the SP of the injected current would be determined also by the injected spin-down current, which should be suppressed for a higher performance of the CFAS—Ge-based spin injection device. In this regard, we carried out a similar analysis for the minority spin-down electrons, as shown in figure 6. For the abrupt i1 structure, the conduction band edges of CFAS and Ge match, which is not desirable as the spin-down electrons would not experience any barrier preventing them from injection into the Ge substrate.

On the other hand, there is a relatively large potential barrier of 0.4 eV in the case of the i2_GeCo structure. This barrier would hinder the injection of spin-down electrons into the substrate, which is beneficial for a higher overall performance of this hybrid interface. These findings suggest opposing effects for the majority and minority electrons. In other words, the abrupt interface is more beneficial for spin-up electron injection, while the interdiffusion interface is more beneficial for spin-down electron suppression. This suggests that a structure with a potential difference between those of these two limiting cases, such as the i1 structure with the interdiffusion of Ge and Fe, would have a higher spin injection efficiency. These findings and reported results suggest that the control of the Fe element at the interface appears to be most important for the realization of higher device performances.

## 4. Conclusion

In this study, the electronic and magnetic properties of CFAS/Ge interfaces were investigated by DFT calculations. In the case of abrupt interfaces, we observed considerable reductions in SP, particularly in the case of the —Fe–Si,Al/Ge interface termination, where the SP has reversed sign. By formation energy analyses, we show that Fe–Ge interdiffusion is most likely to occur at the interface, and that this intermixing does not largely affect the spin-electronic properties. On the contrary, the interdiffusion affecting the Co sublattice in the CFAS film reverses the SP at the interface layers, but it is less likely to occur owing to the higher energy for such atomic swaps. Notably, according to the band alignment analyses, interfaces with a small degree of Fe/Ge intermixing may be even beneficial for the spin injection efficiency. The unexpected potentially beneficial intermixing between Fe and Ge is limited to these systems, and is not expected to be beneficial if, instead of a Co-based Heusler electrode, a standard ferromagnetic electrode such as Fe, Co, CoFe, or CoFeB is used. Additional studies may include consideration of a considerably larger interface region of mixed atomic species in both film and substrate, addressing the phenomena that usually occur if high-temperature annealing or growth is performed. Furthermore, the interfacial properties of other half-metallic Heusler alloys and oxides with technologically important semiconducting structures including Si, GaAs, and InAs as a function of the growth direction, strain effects, and intermixing should be explored.

## Data availability statement

All data that support the findings of this study are included within the article (and any supplementary files).

## Acknowledgments

The Viking cluster was used during this project, which is a high-performance compute facility provided by the University of York. We are grateful for the computational support from the University of York, IT Services and Research IT team. We also acknowledge the support by EPSRC (Grant Number EP/S033394/1).

## ORCID iD

Zlatko Nedelkoski https://orcid.org/0009-0002-3266-9836

## References

[1] Hirohata A and Lloyd D C 2022 *MRS Bull.* **47** 593
[2] Katsnelson M I, Irkhin V Y, Chioncel L, Lichtenstein A I and de Groot R A 2008 *Rev. Mod. Phys.* **80** 315
[3] Xie Y, Zhang S-Y, Yin Y, Zheng N, Ali A, Younis M, Ruan S and Zeng Y-J 2025 *npj Spintronics* **3** 10
[4] Kharel P, Baker G, Wieberdink M, Diallo S, Anas M, Shand P M and Lukashev P V 2024 *J. Appl. Phys.* **57** 375001
[5] Achinuq B *et al* 2018 *Phys. Rev. B* **98** 115304
[6] Yamada A, Yamada M, Kusumoto S, Nascimento J A, Murrill C, Yamada S, Sawano K, Lazarov V K and Hamaya K 2024 *Mater. Sci. Semicond. Process.* **173** 108140
[7] Shan R, Sukegawa H, Wang W H, Kodzuka M, Furubayashi T, Ohkubo T, Mitani S, Inomata K and Hono K 2009 *Phys. Rev. Lett.* **102** 246601
[8] Ishikawa T, Marukame T, Kijima H, Matsuda K-I, Uemura T, Arita M and Yamamoto M 2006 *Appl. Phys. Lett.* **89** 192505
[9] Lari L *et al* 2014 *J. Phys. D: Appl. Phys.* **47** 322003
[10] Sakuraba Y, Hattori M, Oogane M, Ando Y, Kato H, Sakuma A, Miyazaki T and Kubota H 2006 *Appl. Phys. Lett.* **88** 192508
[11] Tsunegi S, Sakuraba Y, Oogane M, Takanashi K and Ando Y 2008 *Appl. Phys. Lett.* **93** 112506
[12] Hamaya K, Hashimoto N, Oki S, Yamada S, Miyao M and Kimura T 2012 *Phys. Rev. B* **85** 100404
[13] Nedelkoski Z, Sanchez A M, Ghasemi A, Hamaya K, Evans R F L, Bell G R, Hirohata A and Lazarov V K 2016 *Appl. Phys. Lett.* **109** 222405
[14] Picozzi S and Freeman A J 2007 *J. Phys.* **19** 315215
[15] Sakuraba Y, Iwase T, Saito K, Mitani S and Takanashi K 2009 *Appl. Phys. Lett.* **94** 012511

[16] Kuerbanjiang B *et al* 2016 *Appl. Phys. Lett.* **108** 172412
[17] Nedelkoski Z, Kepaptsoglou D, Ghasemi A, Kuerbanjiang B, Hasnip P J, Yamada S, Hamaya K, Ramasse Q M, Hirohata A and Lazarov V K 2016 *J. Phys.: Condens. Matter* **28** 395003
[18] Schmidt G, Ferrand D, Molenkamp L W, Filip A T and van Wees B J 2000 *Phys. Rev. B* **62** R4790
[19] Nedelkoski Z *et al* 2016 *Sci. Rep.* **6** 37282
[20] Hamaya K, Fujita Y, Yamada M, Kawano M, Yamada S and Sawano K 2018 *J. Phys. D: Appl. Phys.* **51** 393001
[21] Hamaya K and Yamada M 2022 *MRS Bull.* **47** 584
[22] Clark S J, Segall M D, Pickard C J, Hasnip P J, Probert M I J, Refson K and Payne M C 2005 *Z. Kristallogr.* **220** 567
[23] Chadov S, Fecher G H, Felser C, Minár J, Braun J and Ebert H 2009 *J. Phys. D: Appl. Phys.* **42** 084002
[24] Hasnip P J, Smith J H and Lazarov V K 2013 *J. Appl. Phys.* **113** 17B106
[25] Al-Allak H M and Clark S J 2001 *Phys. Rev. B* **63** 033311
[26] Morris A J, Nicholls R J, Pickard C J and Yates J R 2014 *Comput. Phys. Commun.* **185** 1477
[27] Momma K and Izumi F 2011 *J. Appl. Crystallogr.* **44** 1272
[28] Hamaya K, Itoh H, Nakatsuka O, Ueda K, Yamamoto K, Itakura M, Taniyama T, Ono T and Miyao M 2009 *Phys. Rev. Lett.* **102** 137204
[29] Yamada M, Kuroda F, Tsukahara M, Yamada S, Fukushima T, Sawano K, Oguchi T and Hamaya K 2020 *NPG Asia Mater.* **12** 47
[30] Elphick K, Frost W, Samiepour M, Kubota T, Takanashi K, Sukegawa H, Mitani S and Hirohata A 2021 *Sci. Technol. Adv. Mater.* **22** 235–71
[31] Glover S E, Saerbeck T, Ghasemi A, Kepaptsoglou D, Ramasse Q M, Yamada S, Hamaya K, Hase T P A, Lazarov V K and Bell G R 2018 *J. Phys.: Condens. Matter* **30** 065801